



## Original Article

## Gamma ray attenuation behaviors and mechanism of boron rich slag/epoxy resin shielding composites

Mengge Dong <sup>a, b, c, d,\*</sup>, Suying Zhou <sup>a</sup>, He Yang <sup>a, b, c, d</sup>, Xiangxin Xue <sup>a, b, c, d</sup><sup>a</sup> Department of Resource and Environment, School of Metallurgy, Northeastern University, Shenyang, 110819, PR China<sup>b</sup> Key Laboratory of Metallurgical Resources Recycling Science, Liaoning Province, Shenyang, 110819, PR China<sup>c</sup> Engineering and Technology Research Center for Boron Resource Comprehensive Development and Application of Liaoning Province, Shenyang, 110819, PR China<sup>d</sup> Liaoning Key Laboratory for Ecologically Comprehensive Utilization of Boron Resources and Materials, Shenyang, 110819, PR China

## ARTICLE INFO

## Article history:

Received 16 February 2023

Received in revised form

21 April 2023

Accepted 27 April 2023

Available online 25 May 2023

## Keywords:

Boron rich slag

Epoxy resin

Gamma ray

Shielding performance

Shielding mechanism

## ABSTRACT

Excellent thermal neutron absorption performance of boron expands the potential use of boron rich slag to prepare epoxy resin matrix nuclear shielding composites. However, shielding attenuation behaviors and mechanism of the composites against gamma rays are unclear. Based on the radiation protection theory, Phy-X/PSD, XCOM, and <sup>60</sup>Co gamma ray source were integrated to obtain the shielding parameters of boron rich slag/epoxy resin composites at 0.015–15 MeV, which include mass attenuation coefficient ( $\mu_t$ ), linear attenuation coefficient ( $\mu$ ), half value thickness layer ( $HVL$ ), electron density ( $N_{eff}$ ), effective atomic number ( $Z_{eff}$ ), exposure buildup factor (EBF) and exposure absorption buildup factor (EABF).  $\mu_t$ ,  $\mu$ ,  $HVL$ ,  $N_{eff}$ ,  $Z_{eff}$ , EBF and EABF are 0.02–7 cm<sup>2</sup>/g, 0.04–17 cm<sup>-1</sup>, 0.045–20 cm, 5–14,  $3 \times 10^{23}$ – $8 \times 10^{23}$  electron/g, 0–2000, and 0–3500. Shielding performance is BS4, BS3, BS3, BS1 in descending order, but worse than ordinary concrete.  $\mu$  and  $HVL$  of BS1–BS4 for <sup>60</sup>Co gamma ray is 0.095–0.110 cm<sup>-1</sup> and 6.3–7.2 cm. Shielding mechanism is main interactions for attenuation gamma ray by BS1–BS4 are elements with higher content or higher atomic number via Photoelectric Absorption at low energy range, and elements with higher content via Compton Scattering and Pair Production in Nuclear Field at middle and higher energy range.

© 2023 Korean Nuclear Society, Published by Elsevier Korea LLC. This is an open access article under the CC BY-NC-ND license (<http://creativecommons.org/licenses/by-nc-nd/4.0/>).

## 1. Introduction

Ludwigite ore is an important boron and iron containing ore in China [1]. Generally, ‘mineral separation-blast furnace smelting’ is the mainstream way to separate boron and iron elements in ludwigite ore and in that way ludwigite utilization is realized [2,3]. During the process a large amount of byproduct—blast furnace slag with high boron content (also known as boron rich slag) is generated. Due to its high boron content, boron rich slag can be used as raw materials of borax/boron acid, and it is a significant man-made ore for boron extraction [1,2]. However, as the boron activity of boron rich slag is low, the process of mineral separation-blast furnace smelting will cause a great deal of resource wasting, valuable elements such as boron, iron and magnesium will be

discharged as boron mud. And the lower content of boron (3.65%) [2], the more amount of boron mud will be discharged. Therefore, green, low-carbon and high-efficiency comprehensive utilization of boron rich slag has become a bottleneck problem for boron industry that highly dependent on the production process of ‘mineral separation-blast furnace smelting’.

Boron has excellent thermal neutron absorption performance, which makes it widely used in neutron shielding field. Boron or its compounds are widely used in conventional shields for thermal neutron [4,5], but they are relative expensive. Therefore, we make the following thoughts: Since boron rich slag is the raw material for boron or its compounds preparation, can we directly use boron rich slag as the filler for thermal neutron shielding? In addition, the problem of low boron activity of boron-rich slag can be eliminated, and then the resource and environment problems in the utilization process can be avoided. Thus we have put forward the idea of directly using boron rich slag in the field of nuclear shielding materials, studied the physical law of interactions between boron rich slag and neutron/gamma ray, obtained the attenuation mechanism

\* Corresponding author. Department of Resource and Environment, School of Metallurgy, Northeastern University, Shenyang, 110819, PR China.

E-mail addresses: [mg\\_dong@163.com](mailto:mg_dong@163.com), [dongmengge@smm.neu.edu.cn](mailto:dongmengge@smm.neu.edu.cn) (M. Dong).

of boron rich slag for gamma ray/neutron, and found that the shielding ability of boron rich slag was better than that of commercial materials [6–8]. Subsequently, it is well known that the epoxy resin has many advantages, e.g. high hydrogen content, excellent processability, strong radiation resistance, suitability for adding a large amount of low-cost shielding fillers and ease of composites preparation. Besides, some researchers had prepared nuclear shielding materials with suitable comprehensive properties by using boron containing ores and epoxy resin matrix [6,9–12]. Therefore, we used epoxy resin as the matrix material to prepare the shielding composites at room temperature with different addition amount of boron rich slag, the results showed that shielding performance of the prepared composites were better than some commercial materials for thermal neutron [2]. Furthermore, the utilization mode as thermal neutron shielding materials not only provides an innovative channel for green, low-carbon and high-efficiency comprehensive utilization of boron rich slag, but also avoids waste of resources and environmental pollution.

However, the interaction between boron/hydrogen and thermal neutron will emit the gamma ray at 0.478 MeV and 2.22 MeV [13–15], respectively, boron and hydrogen are the main compositions in the prepared composites. Attention should be paid to this special phenomenon to avoid potential hazards from secondary gamma rays when use the prepared shielding composites. In our previous work vanadium slag can be used as filler to improve the gamma ray shielding performance [16], but the shielding attenuation behaviors and mechanism of boron rich slag/epoxy resin composites against gamma rays are unclear. Therefore, the key point of this paper is to obtain the gamma ray shielding behaviors and analyze the shielding attenuation mechanism of the prepared composites.

When narrow beam gamma rays pass through the shield, Lambert-Beer law ( $I=I_0 \cdot e^{-\mu t}$ ) can be used to describe the transmission process, where  $I$  and  $I_0$  are transmitted and initial photon densities,  $\mu$  is linear attenuation coefficient ( $\text{cm}^{-1}$ ) and  $t$  is the thickness of medium [17]. Besides, mass attenuation coefficient ( $\mu_t$ ,  $\text{cm}^2/\text{g}$ ), linear attenuation coefficient, half value thickness layer ( $HVL$ ,  $\text{cm}$ ), electron density ( $N_{\text{eff}}$ , electron/g) and effective atomic number ( $Z_{\text{eff}}$ ) are important shielding parameters to describe the shielding behaviors [7,17–19]. However, the actual gamma ray is often in the form of a wide beam, while the buildup factor ( $B$ ) is used to modify the Lambert-Beer law as  $I=B \cdot I_0 \cdot e^{-\mu \cdot t}$ , thus exposure buildup factor (EBF) and exposure absorption buildup factor (EABF) are key parameters for wide beam gamma ray shielding performance [8,20–24].

Therefore, boron rich slag/epoxy resin nuclear shielding composites with excellent thermal neutron protection performance is studied in this paper. Based on the radiation protection theory, Phy-X/PSD program, XCOM program, and  $^{60}\text{Co}$  gamma ray source were integrated to obtain the shielding parameters of boron rich slag/epoxy resin composites at 0.015–15 MeV, which include mass attenuation coefficient ( $\mu_t$ ), linear attenuation coefficient ( $\mu$ ), half value thickness layer ( $HVL$ ), electron density ( $N_{\text{eff}}$ ), effective atomic number ( $Z_{\text{eff}}$ ), exposure buildup factor (EBF) and exposure absorption buildup factor (EABF), and then the shielding mechanism was revealed. Thus the obtained shielding behaviors and shielding mechanism are the most important novelty of this paper. Moreover, the work is important for the application of the boron rich slag in the nuclear shielding field, especially for the thermal neutron shields.

## 2. Materials and methods

### 2.1. Materials

In this work, the preparation process and compositions of the boron rich slag/epoxy resin nuclear shielding composites (BS1-BS4)

was the same with our past work [2]. The raw materials in this investigation were Epoxy resin (E-51, Blue Star Chemical New Material Co. Limited, Nanjing, China), polyamide resin (651, Blue Star Chemical New Material Co. Limited, Nanjing, China), and boron bearing blast furnace slag (B<sup>3</sup>FS) (Liaoning Fengcheng Iron and Steel Co. Limited, Liaoning, China). Macroscopic picture of BS1-BS4 was shown in Fig. S1. While the measured densities of BS1-BS4 are 1.649 g/cm<sup>3</sup>, 1.869 g/cm<sup>3</sup>, 2.037 g/cm<sup>3</sup> and 2.134 g/cm<sup>3</sup>, respectively. The chemical compositions of BS1-BS4 were shown in Table 1. Moreover, Tables S1 and S2 illustrate the chemical compositions and densities of boron rich slag and epoxy resin.

### 2.2. Calculation for gamma ray shielding parameters

In this paper, Phy-X/PSD program, the most friendly analysis software in gamma ray analysis at present, which can be used to analyze the shielding parameters of complex shields, was used to calculate mass attenuation coefficient ( $\mu_t$ ,  $\text{cm}^2/\text{g}$ ), linear attenuation coefficient ( $\mu$ ,  $\text{cm}^{-1}$ ), half value thickness layer ( $HVL$ ,  $\text{cm}$ ), electron density ( $N_{\text{eff}}$ , electron/g), effective atomic number ( $Z_{\text{eff}}$ ), exposure buildup factor (EBF) and exposure absorption buildup factor (EABF) at 0.015–15 MeV [25,26]. Besides, XCOM program

**Table 1**  
Chemical compositions of BS1-BS4.

Element	Sample (wt %)			
	BS1	BS2	BS3	BS4
C	0.3111	0.2392	0.2007	0.1767
H	0.0433	0.0302	0.0232	0.0188
O	0.3047	0.3398	0.3587	0.3705
N	0.0113	0.0079	0.0061	0.0049
B	0.0238	0.0277	0.0297	0.031
Mg	0.1374	0.1596	0.1715	0.1789
Si	0.0702	0.0815	0.0876	0.0914
Fe	0.0052	0.006	0.0064	0.0067
Al	0.0243	0.0282	0.0303	0.0316
Ca	0.0687	0.0799	0.0858	0.0895



Fig. 1.  $^{60}\text{Co}$  gamma ray test device.

(NIST) could be used to calculate the partial and total attenuation coefficient of the shielding materials, e.g. Photoelectron Absorption, Coherent Scattering, Incoherent Scattering, Pair Production in Nuclear Field, Pair Production in Electron Field, thus it was used to analyze the partial and total attenuation coefficient of the prepared samples [27,28].

### 2.3. Shielding test for gamma ray

The gamma ray shielding was tested by  $\text{a}^{60}\text{Co}$  (1.25 MeV, 5000 Ci) gamma ray source with Unidos dosimeter (PTW, Germany, 30 cc) and 2571 ionization chamber (NE, American) as shown in Fig. 1. Thickness of the prepared samples is about 0.5 cm. Then the linear attenuation coefficient and half value thickness were obtained as Eq. (1) and (2).

$$\mu = -\frac{\ln(I/I_0)}{t} \quad (1)$$

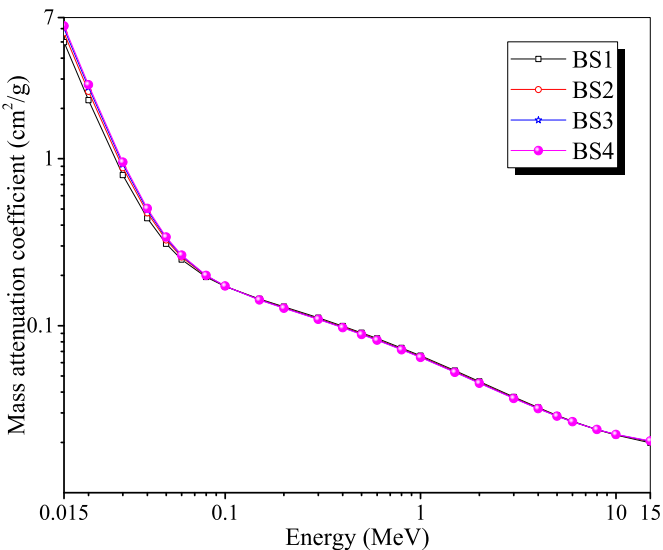


Fig. 2. Mass attenuation coefficients of BS1-BS4 at 0.015–15 MeV.

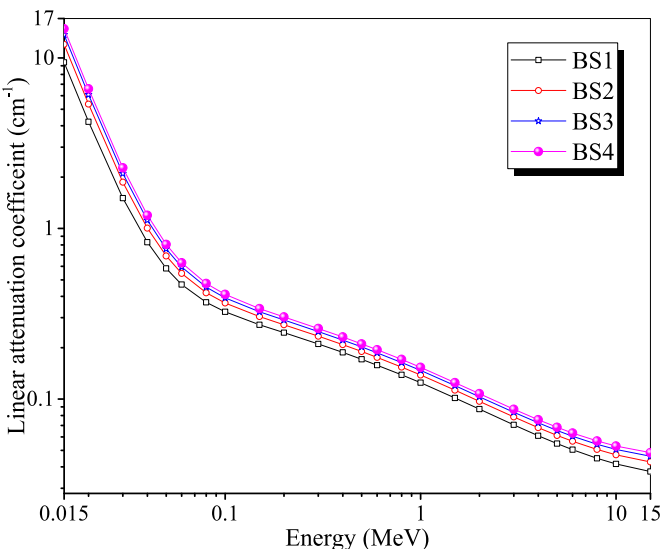


Fig. 3. Linear attenuation coefficients of BS1-BS4 at 0.015–15 MeV.

$$HVL = \frac{\ln 2}{\mu} \quad (2)$$

Where  $I$  and  $I_0$  means the counts of the detector with/without shield, and  $t$  is the thickness (cm) of the shield.

## 3. Results and discussions

### 3.1. Shielding parameters of BS1-BS4 for narrow beam gamma ray

Fig. 2 shows the mass attenuation coefficients of BS1-BS4 at 0.015–15 MeV, it can be seen that the mass attenuation coefficients of BS1-BS4 decrease with the increase of the gamma ray energy. At 0.001–0.08 MeV, the mass attenuation coefficient decreases significantly, which is proportional to  $Z^{4.5}$  [29]. Then it decreases slightly with the increase of the gamma ray energy at 0.1–6 MeV, where it is proportional to  $Z$  [29]. Besides, the mass attenuation

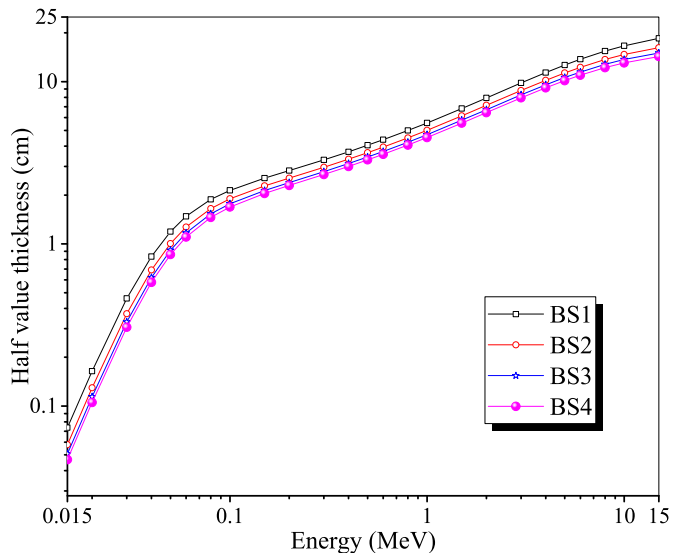


Fig. 4. Half value thickness of BS1-BS4 at 0.015–15 MeV.

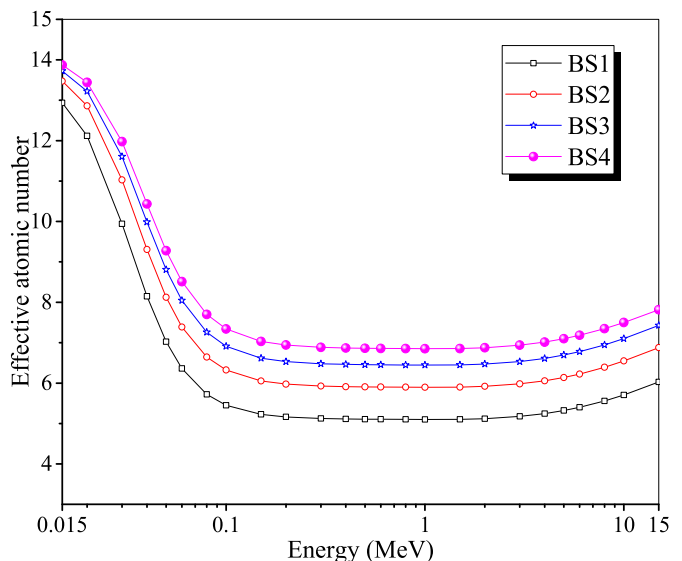


Fig. 5. Effective atomic number of BS1-BS4 at 0.015–15 MeV.

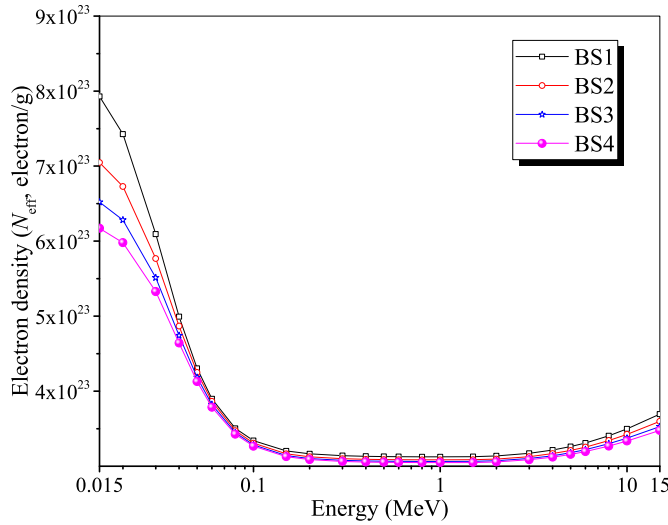


Fig. 6. Electron density of BS1-BS4 at 0.015–15 MeV.

coefficients decrease weakly with the energy range at 6–15 MeV, which is proportional to  $Z^2$  [29]. In addition, the mass attenuation coefficients of BS1-BS4 are 0.02–7  $\text{cm}^2/\text{g}$ , which have significant differences at 0.001–0.08 MeV, and nearly the same at 0.08–15 MeV, values of the mass attenuation coefficient of the prepared samples are BS4, BS3, BS2, BS1 in descending order.

**Fig. 3** is the linear attenuation coefficients of BS1-BS4 at 0.015–15 MeV, it is in a same trend with mass attenuation coefficients as shown in **Fig. 2**, where it decreases significantly at 0.001–0.08 MeV, slightly at 0.1–6 MeV, and more weakly at 6–15 MeV. However, it can be significantly distinguished the values of the linear attenuation coefficient at 0.015–15 MeV. Besides, the linear attenuation coefficient of BS1-BS4 is 0.04–17  $\text{cm}^{-1}$ , and shielding ability of the prepared composites are BS4, BS3, BS2, BS1 in descending order.

**Fig. 4** is the half value thickness of BS1-BS4 at 0.015–15 MeV, it is in a opposite variation with both the mass attenuation coefficient (**Fig. 2**) and linear attenuation coefficient (**Fig. 3**), where it increases significantly at 0.001–0.08 MeV, slightly at 0.1–6 MeV, and more weakly at 6–15 MeV. In addition, the half value thickness of BS1-BS4 is 0.045–20 cm. Moreover, it can be significantly distinguished for the values of the half value thickness of BS1-BS4 at the whole energy range, where the half value thickness is BS1, BS2, BS3, BS4 in descending order.

**Fig. 5** and **Fig. 6** illustrate the effective atomic number and electron density of BS1-BS4 at 0.015–15 MeV, it can be seen that the two parameters are in the same variation with the gamma ray energy at 0.015–15 MeV. While the effective atomic number and electron density of BS1-BS4 decrease rapidly at 0.015–0.15 MeV, nearly the same at 0.15–3 MeV, and increase slowly at 3–15 MeV. Besides, the lowest value is appeared at the energy range of 0.15–3 MeV. Also the effective atomic number of the BS1-BS4 is 5–14, and the electron density is  $3 \times 10^{23}$ – $8 \times 10^{23}$  electron/g.

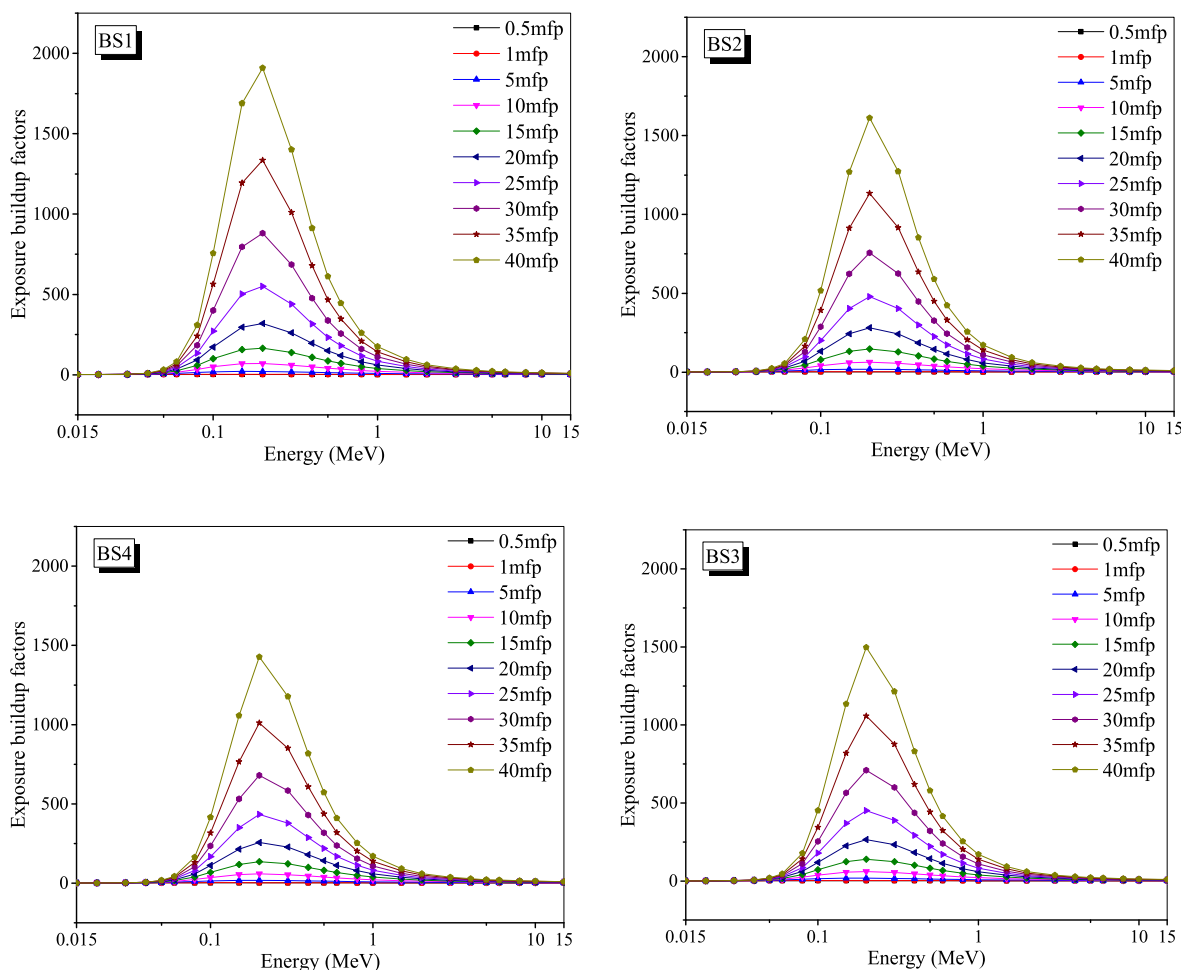


Fig. 7. Exposure buildup factors of BS1-BS4 at 0.015–15 MeV.

What's more, it can be clearly seen the effective atomic number of the prepared composites is BS4, BS3, BS3, BS1 in descending order, but the electron density is in an opposite variation, especially at low and high gamma ray energy range.

The reason for the parameters' variation can be concluded as follow: Photoelectric Absorption is dominant attenuation effect at low energy region, Compton Scattering is dominant attenuation effect at middle energy region, and Pair Production is dominant attenuation effect at high energy region [27,28]. Furthermore, it is precisely due to the changes in types of the above-mentioned nuclear reactions and components that the variation of parameters described above. At the same time, according to the definition of the parameters, the shielding performance of the prepared composites is BS4, BS3, BS3, BS1 in descending order.

### 3.2. Exposure buildup factors and energy absorption buildup factors

**Fig. 7** and **Fig. 8** are the exposure buildup factors and exposure absorption buildup factors of BS1–BS4 at 0.015–15 MeV, respectively. These two figures indicate that the exposure buildup factors and exposure absorption buildup factors are in the same variation with the increase of the gamma ray energy, where they are nearly the same at 0.015–0.05 MeV and 3–15 MeV, increase rapidly at 0.05–0.2 MeV, and decrease rapidly at 0.2–3 MeV, while the highest value is at 0.2 MeV and lowest value is in the energy range of 0.015–0.05 MeV and 3–15 MeV. Exposure buildup factors are 0–2000, and exposure absorption buildup factors are 0–3500. In addition, exposure buildup factors and exposure absorption

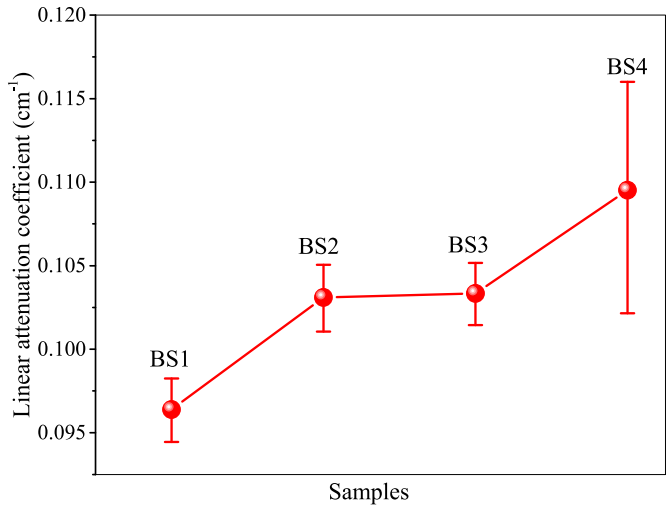


**Fig. 9.** Linear attenuation coefficients of BS1–BS4 for  $^{60}\text{Co}$  gamma ray.

buildup factors increase with the penetration depth. However, the main interactions between the gamma ray matter is Photoelectric Absorption at low energy range, Compton Scattering at middle energy range, and Pair Production at high energy range, while the buildup factors reflect the influence of the scattering effect through the transmission process, thus the variation is significant at middle energy range [27,28,30–32]. Moreover, the thicker the penetration

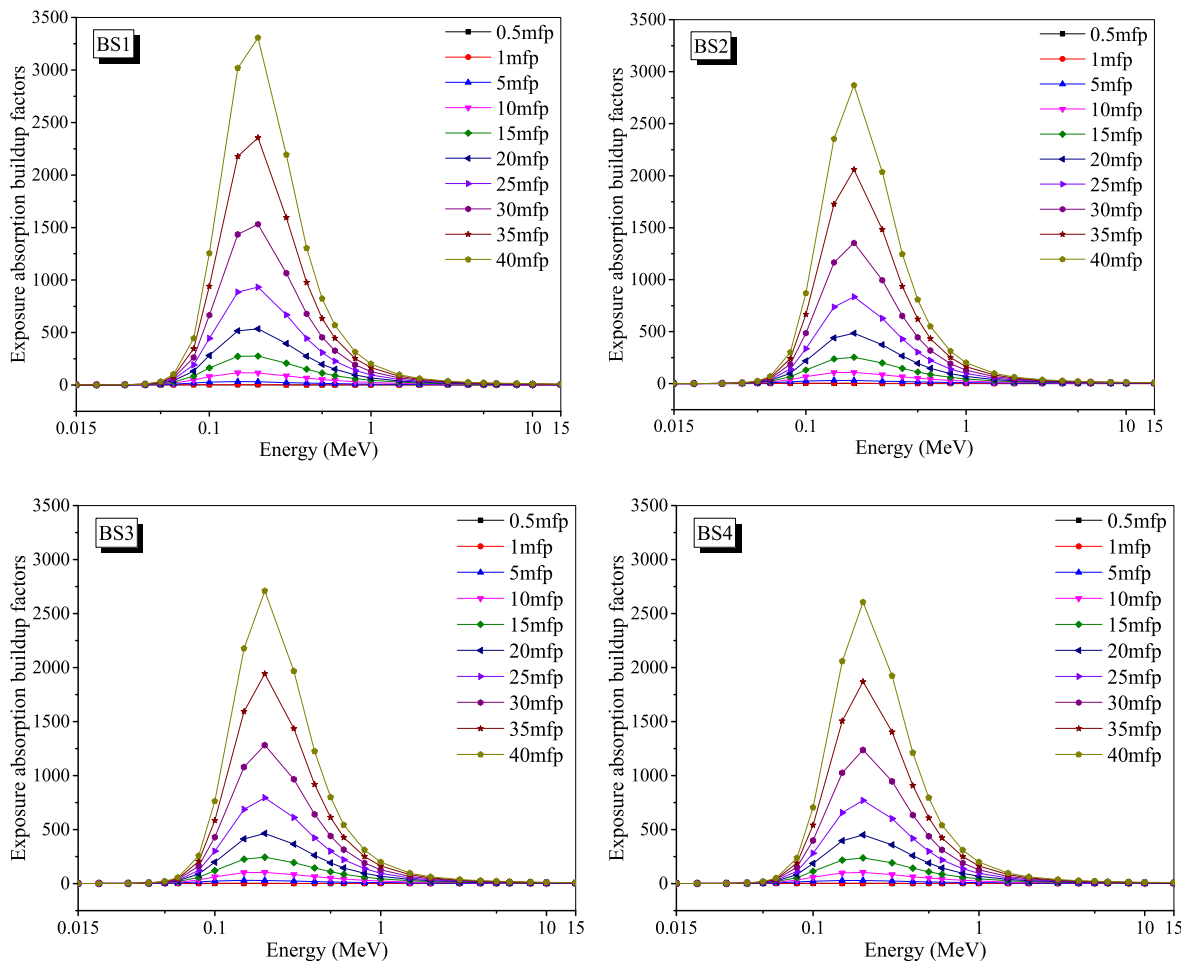


**Fig. 8.** Exposure absorption buildup factors of BS1–BS4 at 0.015–15 MeV.

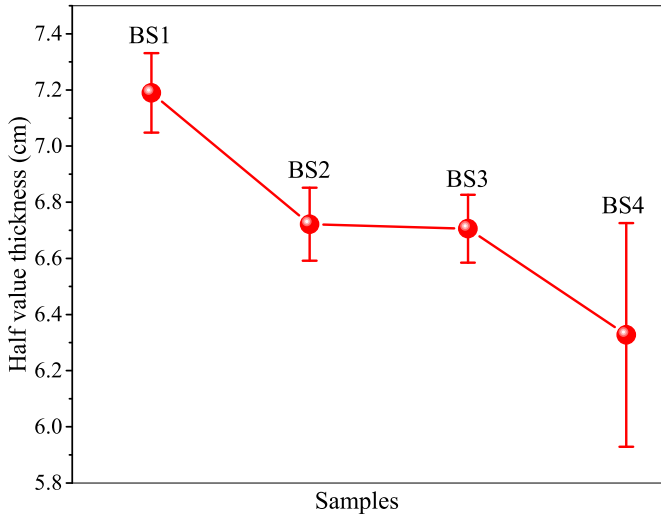


Fig. 10. Half value thickness of BS1-BS4 for  $^{60}\text{Co}$  gamma ray.

depth, the scattering effect will be more complex, and it causes the increase of the buildup factors [33].

### 3.3. Test results

Fig. 9 and Fig. 10 illustrate the linear attenuation coefficient and half value thickness of BS1-BS4 for  $^{60}\text{Co}$  gamma ray, it can be seen that the linear attenuation coefficient of BS1-BS4 increases from

BS1-BS4, and the half value thickness decrease from BS1 to BS4. Linear attenuation coefficient is between 0.095 and  $0.110\text{ cm}^{-1}$ , half value thickness is between 6.3 and 7.2 cm. Besides, the higher linear attenuation coefficient/lower half value thickness means better shielding performance. Moreover, comparison of linear attenuation coefficient of BS1-BS4 between the test results and theoretical results for  $^{60}\text{Co}$  gamma ray is shown in Table S3, the relative error is between 1.11%–12.43%. Fig. S2 illustrates the comparison of the shielding performance of BS1-BS4, epoxy resin and some concrete shields [34], shielding performance of BS1-BS4 is better than epoxy resin matrix because the shielding performance of born rich slag is always better than epoxy resin matrix as shown in Fig. S3. However, the shielding performance of BS1-BS4 is even worse than the ordinary concrete.

### 3.4. Shielding mechanism for gamma ray

Fig. 11 is the partial and total mass attenuation coefficients of BS1-BS4 at 0.015–15 MeV, it indicates the interactions of BS1-BS4 and gamma rays are Photoelectric Absorption, Compton Scattering, and Pair Production in Nuclear Field at high energy range, while Coherent Scattering and Paid Production in electron Field have a little influence on the total mass attenuation coefficient. At 0.015–0.02 MeV, the Photoelectric Absorption is the main interaction; With the increase of the energy, the effect of Compton Scattering and Coherent Scattering increases, and the effect of Photoelectric Absorption decreases; At 0.15–3 MeV, the main interaction is Compton Scattering. Effect of the Compton Scattering decreases, and the Pair Production in Nuclear Field increases with

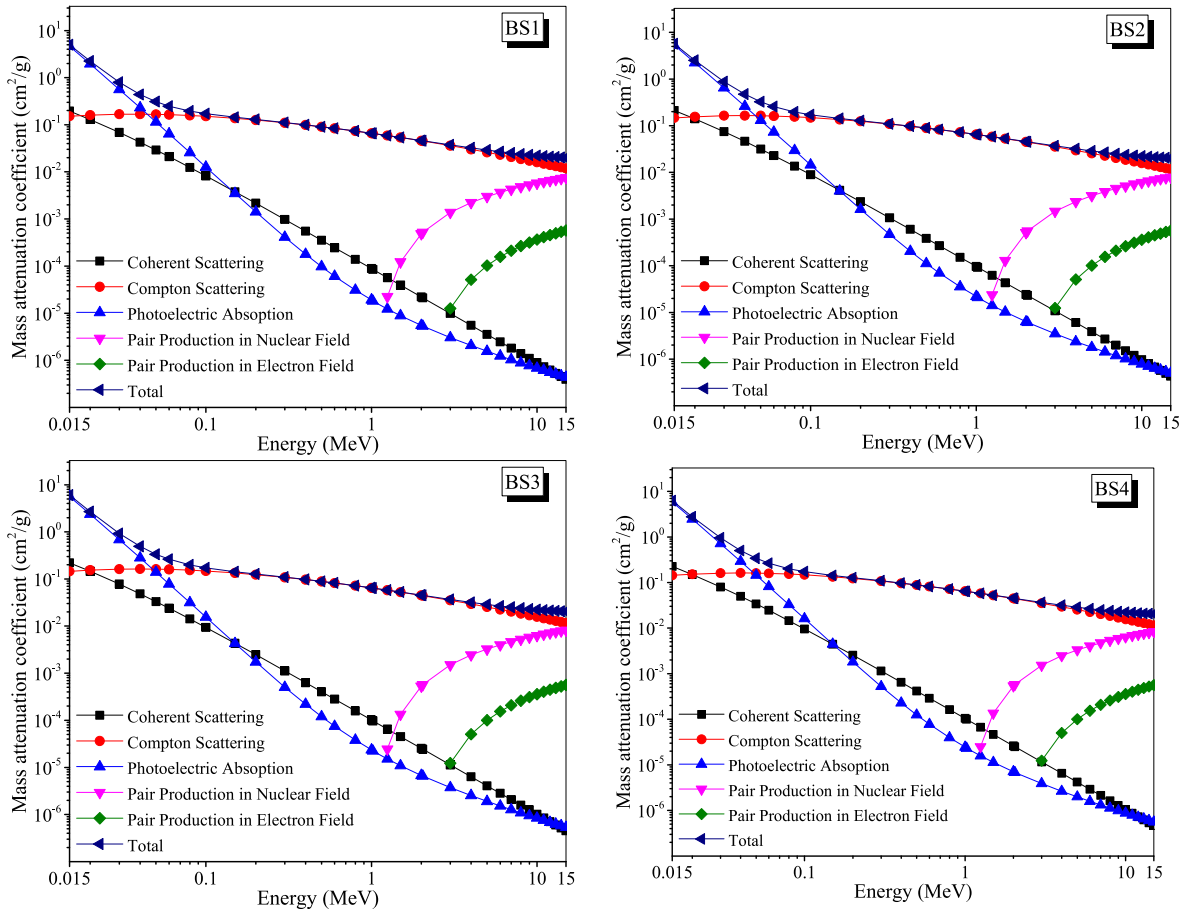
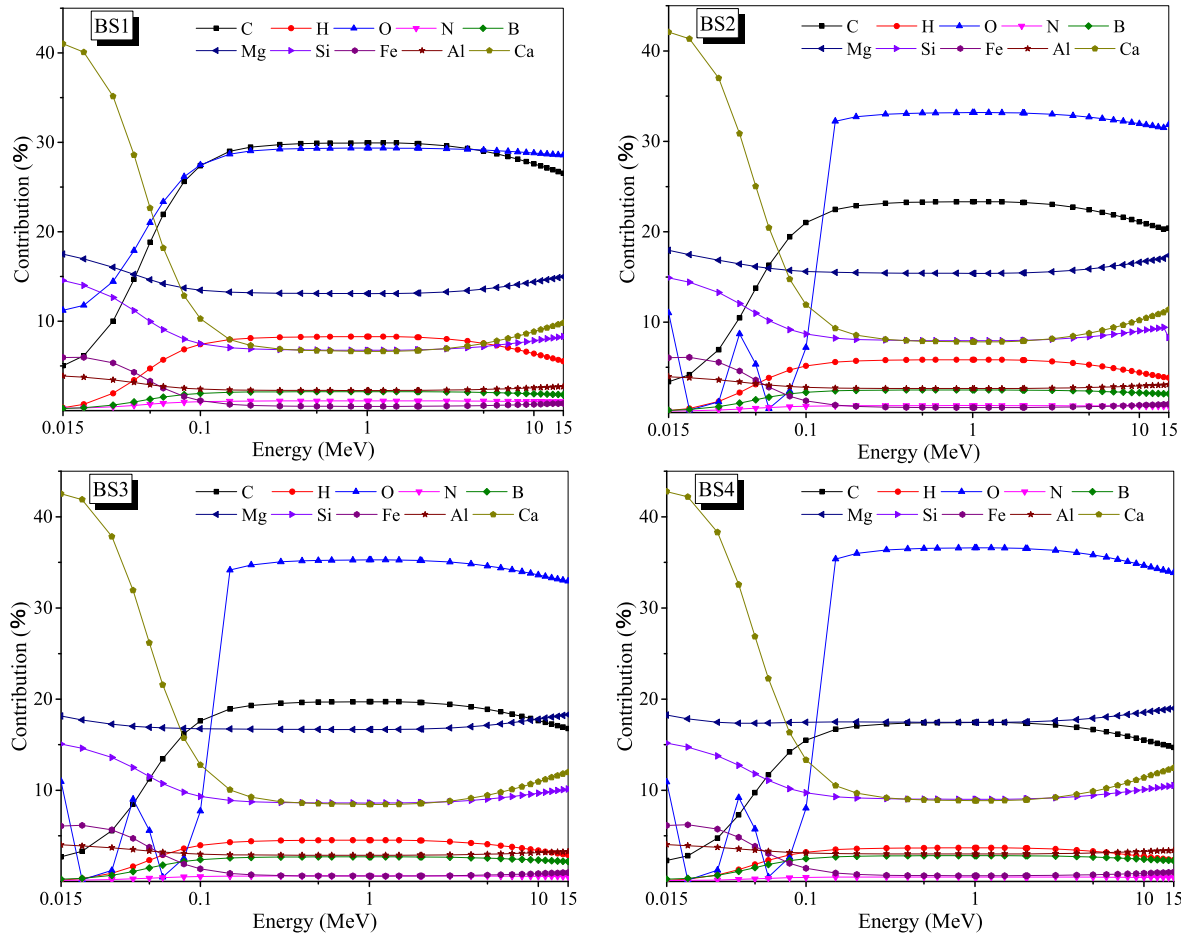


Fig. 11. Partial and total mass attenuation coefficients of BS1-BS4 at 0.015–15 MeV.



**Fig. 12.** Contribution of elements in BS1-BS4 for shielding performance at 0.015–15 MeV.

the variation of the energy range at 3–15 MeV, also the Paid Production in Electron field affect a little on the total mass attenuation coefficient.

Fig. 12 shows the contribution of elements in BS1-BS4 for shielding performance at 0.015–15 MeV, the contribution of each element is in the same variation with the increase of energy, except for the O in BS1. Besides, the contribution of each element for BS1-BS4 is different due to the content of each element. However, elements with higher atomic number and relatively higher content may have main contribution in the low energy region (e.g. Ca), and the higher content elements make a significant contribution (e.g. O and C). With the energy increases up to 15 MeV, the elements with higher content show main contribution for the total mass attenuation coefficient, and the elements with higher atomic number and relative higher content show the important contribution. In conclusion, the main interactions for gamma ray attenuation by BS1-BS4 are the elements with higher content or higher atomic number via Photoelectric Absorption at low energy range, and the elements with higher content via Compton Scattering and Pair Production in Nuclear Field at middle and higher energy range.

#### 4. Conclusions

Mass attenuation coefficient ( $\mu_t$ ), linear attenuation coefficient ( $\mu$ ), half value thickness layer ( $HVL$ ), electron density ( $N_{eff}$ ), effective atomic number ( $Z_{eff}$ ), exposure buildup factor (EBF) and exposure absorption buildup factor (EABF) of boron rich slag/epoxy resin nuclear shielding composites (BS1-BS4) at 0.015–15 MeV are

0.02–7  $\text{cm}^2/\text{g}$ , 0.04–17  $\text{cm}^{-1}$ , 0.045–20  $\text{cm}$ , 5–14,  $3 \times 10^{23}$ – $8 \times 10^{23}$   $\text{electron/g}$ , 0–2000, and 0–3500, respectively. Shielding performance of the prepared composites is BS4, BS3, BS1 in descending order.  $\mu$  and  $HVL$  of BS1-BS4 for  $^{60}\text{Co}$  gamma ray is 0.095–0.110  $\text{cm}^{-1}$  and 6.3–7.2 cm, respectively. Shielding mechanism is that the main interactions for gamma ray attenuation by BS1-BS4 are the elements with higher content or higher atomic number via Photoelectric Absorption at low energy range, and the elements with higher content via Compton Scattering and Pair Production in Nuclear Field at middle and higher energy range. The work is meaningful for the potential application of the boron rich slag in the nuclear shielding field.

#### CRediT authorship contribution statement

**Mengge Dong:** Supervision; Conceptualization; Methodology; Software; Project administration; Funding acquisition. **Suying Zhou:** Formal analysis; Investigation; Writing - Original Draft. **He Yang:** Supervision; Funding acquisition. **Xiangxin Xue:** Project administration; Funding acquisition.

#### Declaration of competing interest

The authors declare that they have no known competing financial interests or personal relationships that could have appeared to influence the work reported in this paper.

## Acknowledgements

This work was supported by National Natural Science Foundation of China (52204417), the Fundamental Research Funds for the Central Universities (N2225036), Postdoctoral Science Foundation of Northeastern University (20210207), and the National key research and development plan of China (2020YFC1909805). The authors thank the reviewers for their comments that improved the manuscript.

## Appendix A. Supplementary data

Supplementary data to this article can be found online at <https://doi.org/10.1016/j.net.2023.04.041>.

## References

- [1] J. An, X. Xue, Life cycle environmental impact assessment of borax and boric acid production in China, *J. Clean. Prod.* 66 (2014) 121–127.
- [2] M. Dong, S. Zhou, X. Xue, X. Feng, H. Yang, M.I. Sayyed, D. Tishkevich, A. Trukhanov, N. Almousa, Upcycling of boron bearing blast furnace slag as highly cost-effective shield for protection of neutron radiation hazard: an innovative way and proposal of shielding mechanism, *J. Clean. Prod.* 355 (2022), 131817.
- [3] J. You, J. Wang, J. Luo, Z. Peng, M. Rao, G. Li, A facile route to the value-added utilization of ludwigite ore: boron extraction and  $M_xMg_{1-x}Fe_{2O_4}$  spinel ferrites preparation, *J. Clean. Prod.* 375 (2022), 134206.
- [4] W. Ramadan, K. Sakr, M. Sayyed, N. Maziad, N. El-Faramawy, Investigation of acrylic/boric acid composite gel for neutron attenuation, *Nucl. Eng. Technol.* 52 (11) (2020) 2607–2612.
- [5] B.M. Chandrika, H.C.S. Manjunatha, K.N. Sridhar, M.R. Ambika, L. Seenappa, S. Manjunatha, et al., Synthesis, physical, optical and radiation shielding properties of Barium-Bismuth Oxide Borate-A novel nanomaterial, *Nucl. Eng. Technol.* 55 (5) (2023) 1783–1790.
- [6] M. Dong, S. Zhou, X. Xue, X. Feng, M.I. Sayyed, M.U. Khandaker, D.A. Bradley, The potential use of boron containing resources for protection against nuclear radiation, *Radiat. Phys. Chem.* 188 (2021), 109601.
- [7] M.G. Dong, X.X. Xue, Y. Elmahroug, M.I. Sayyed, M.H.M. Zaid, Investigation of shielding parameters of some boron containing resources for gamma ray and fast neutron, *Results Phys.* 13 (2019), 102129.
- [8] M.G. Dong, X.X. Xue, V.P. Singh, H. Yang, Z.F. Li, M.I. Sayyed, Shielding effectiveness of boron-containing ores in Liaoning province of China against gamma rays and thermal neutrons, *Nucl. Sci. Tech.* 29 (4) (2018) 1–8.
- [9] K. Okuno, Neutron shielding material based on colemanite and epoxy resin, *Radiat. Protect. Dosim.* 115 (1–4) (2005) 258–261.
- [10] M. Dong, X. Xue, Z. Li, H. Yang, M.I. Sayyed, B.O. Elbashir, Preparation, shielding properties and mechanism of a novel neutron shielding material made from natural Szaibelyite resource, *Prog. Nucl. Energy* 106 (2018) 140–145.
- [11] M. Dong, X. Xue, S. Liu, H. Yang, Z. Li, M.I. Sayyed, O. Agar, Using iron concentrate in Liaoning Province, China, to prepare material for X-Ray shielding, *J. Clean. Prod.* 210 (2019) 653–659.
- [12] M. Dong, S. Zhou, X. Xue, M.I. Sayyed, D. Tishkevich, A. Trukhanov, C. Wang, Study of comprehensive shielding behaviors of chambersite deposit for neutron and gamma ray, *Prog. Nucl. Energy* 146 (2022), 104155.
- [13] I. Kanno, D. Nishimatsu, F. Funama, Simulation study on the feasibility of current-mode SPECT for B-10 concentration estimation in boron neutron capture therapy, *J. Instrum.* 14 (2) (2019), C02002.
- [14] M. Chin, N. Spyrou, Monitoring of gamma emission and neutron transmission during boron neutron capture treatment delivery, *J. Radioanal. Nucl. Chem.* 281 (1) (2009) 149–152.
- [15] D.Y. Shu, C.R. Geng, X.B. Tang, C.H. Gong, W.C. Shao, Y. Ai, Analysis on the emission and potential application of Cherenkov radiation in boron neutron capture therapy: a Monte Carlo simulation study, *Appl. Radiat. Isot.* 137 (2018) 219–224.
- [16] M. Dong, X. Xue, H. Yang, Z. Li, Highly cost-effective shielding composite made from vanadium slag and boron-rich slag and its properties, *Radiat. Phys. Chem.* 141 (2017) 239–244.
- [17] T. Kaur, J. Sharma, T. Singh, Experimental evaluation of gamma rays shielding parameters for Zn-Cd-Sn-Pb quaternary alloy, *Radiat. Phys. Chem.* 156 (2019) 193–198.
- [18] M.I. Sayyed, A. Kumar, H.O. Tekin, R. Kaur, M. Singh, O. Agar, M.U. Khandaker, Evaluation of gamma-ray and neutron shielding features of heavy metals doped  $Bi_2O_3$ -Ba-O-Na<sub>2</sub>O-MgO-B<sub>2</sub>O<sub>3</sub> glass systems, *Prog. Nucl. Energy* 118 (2020), 103118.
- [19] A. Sharma, M.I. Sayyed, O. Agar, H.O. Tekin, Simulation of shielding parameters for  $TeO_2$ - $WO_3$ - $GeO_2$  glasses using FLUKA code, *Results Phys.* 13 (2019), 102199.
- [20] M.I. Sayyed, M.Y. AlZaatreh, M.G. Dong, M.H.M. Zaid, K.A. Matori, H.O. Tekin, A comprehensive study of the energy absorption and exposure buildup factors of different bricks for gamma-rays shielding, *Results Phys.* 7 (2017) 2528–2533.
- [21] M.I. Sayyed, Y. Elmahroug, B.O. Elbashir, S.A. Issa, Gamma-ray shielding properties of zinc oxide soda lime silica glasses, *J. Mater. Sci. Mater. Electron.* 28 (2017) 4064–4074.
- [22] O. Agar, E. Kavaz, E.E. Altunsoy, O. Kilicoglu, H.O. Tekin, M.I. Sayyed, T.T. Erguzel, N. Tarhan,  $Er_2O_3$  effects on photon and neutron shielding properties of  $TeO_2$ - $Li_2O$ - $ZnO$ - $Nb_2O_5$  glass system, *Results Phys.* 13 (2019), 102277.
- [23] M.H.A. Mhareb, Y. Slimani, Y.S. Alajerami, M.I. Sayyed, E. Lacomme, M.A. Almessiere, Structural and radiation shielding properties of  $BaTiO_3$  ceramic with different concentrations of Bismuth and Ytterbium, *Ceram. Int.* 46 (18) (2020) 28877–28886.
- [24] M.I. Sayyed, M.H.A. Mhareb, Y.S.M. Alajerami, K.A. Mahmoud, M.A. Imheidad, F. Alshahri, M. Alqahtani, T. Al-Abdullah, Optical and radiation shielding features for a new series of borate glass samples, *Optik* 239 (2021), 166790.
- [25] E. Şakar, Ö.F. Özpolat, B. Alim, M.I. Sayyed, M. Kurudirek, Phy-X/PSD: development of a user friendly online software for calculation of parameters relevant to radiation shielding and dosimetry, *Radiat. Phys. Chem.* 166 (2020), 108496.
- [26] Y. Al-Hadeethi, M.I. Sayyed, Radiation attenuation properties of  $Bi_2O_3$ - $Na_2O$ - $V_2O_5$ - $TiO_2$ - $TeO_2$  glass system using Phy-X/PSD software, *Ceram. Int.* 46 (4) (2020) 4795–4800.
- [27] M.J. Berger, J.H. Hubbell, XCOM: Photon Cross Sections on a Personal Computer (No. NBSIR-87-3597), National Bureau of Standards, Washington, DC (USA), 1987 (Center for Radiation Research).
- [28] L. Gerward, N. Guillet, K.B. Jensen, H. Levring, X-ray absorption in matter, *Reeng. XCOM. Radiat. Phys. Chem.* 60 (1–2) (2001) 23–24.
- [29] R.C. Murty, Effective atomic numbers of heterogeneous materials, *Nature* 207 (4995) (1965) 398–399.
- [30] Y. Harima, An approximation of gamma-ray buildup factors by modified geometrical progression, *Nucl. Sci. Eng.* 83 (2) (1983) 299–309.
- [31] Y. Harima, Y. Sakamoto, S. Tanaka, M. Kawai, Validity of the geometric-progression formula in approximating gamma-ray buildup factors, *Nucl. Sci. Eng.* 94 (1) (1986) 24–35.
- [32] ANSI/ANS-6.4.3, Gamma Ray Attenuation Coefficient and Buildup Factors for Engineering Materials [S], American Nuclear Society, La Grange Park, Illinois, 1991.
- [33] D.K. Gaikwad, S.S. Obaid, M.I. Sayyed, R.R. Bhosale, V.V. Awasarmol, A. Kumar, M.D. Shirsat, P.P. Pawar, Comparative study of gamma ray shielding competence of  $WO_3$ - $TeO_2$ - $PbO$  glass system to different glasses and concretes, *Mater. Chem. Phys.* 213 (2018) 508–517.
- [34] I.I. Bashter, Calculation of radiation attenuation coefficients for shielding concretes, *Ann. Nucl. Energy* 24 (17) (1997) 1389–1401.